

Reconstruction of the second layer of Ag on Pt(111)

Raghani Pushpa

Center for Probing the Nanoscale, Stanford University, Stanford, California 94305, USA

Javier Rodríguez-Laguna

Dpto. Matemáticas, Universidad Carlos III de Madrid, Madrid 28911, Spain

Silvia N. Santalla

Dpto. Física, Universidad Carlos III de Madrid, Madrid 28911, Spain

(Dated: October 15, 2008)

The reconstruction of an Ag monolayer on Ag/Pt(111) is analysed theoretically, employing a vertically extended Frenkel-Kontorova model whose parameters are derived from density functional theory. Energy minimization is carried out using simulated quantum annealing techniques. Our results are compatible with the STM experiments, where a striped pattern is initially found which transforms into a triangular reconstruction upon annealing. In our model we recognize the first structure as a metastable state, while the second one is the true energy minimum.

PACS numbers: 68.35.Bs, 61.72.Bb, 68.35.Md, 68.55.-a, 02.60.Pn

I. INTRODUCTION

One of the most important physical processes that must be properly understood in order to manufacture the nanoscale devices is surface reconstruction, i.e., the morphology changes in the epilayer of a material as a result of reduced coordination, either in homoepitaxial or heteroepitaxial systems. The lattice parameter of the epilayer is usually different from that of the bulk system, giving rise to surface stress. This stress can be relieved in a variety of ways, inducing the appearance of interesting patterns^{1,2,3}.

In this work we analyse the reconstruction of the second monolayer (ML) of Ag deposited on a clean surface of Pt(111). The experiments of Brune and coworkers^{4,5} show that, while the first ML is pseudomorphic (i.e., copies the structure of Pt(111)), the second monolayer reconstructs in a striped pattern, which upon annealing at 800 K, gives rise to an intricate trigonal network, reminiscent of a kagome lattice. Along (111) direction, silver presents a lattice parameter of $a_{\text{Ag}} = 2.95 \text{ \AA}$, which is 4% higher than that of platinum, $a_{\text{Pt}} = 2.83 \text{ \AA}$.

Henceforth, we will refer to the system composed of a complete first monolayer (ML) of Ag on Pt(111) as Ag/Pt(111). Ag atoms in the second ML on that structure can stay in two types of local minima, both arranged in triangular networks, which are denoted as FCC and HCP sites (Figure 1). Earlier work^{6,7} has shown that the two types of sites have very similar energies, being the FCC site favoured by 3 meV. In the middle point of the segment connecting a FCC and a HCP site there is a *bridge* saddle-point site. The energy of an Ag atom in the second ML at the bridge site constitutes the energy barrier to jump from one type of minimum to the other. It was estimated by a theoretical fitting of experimental data on island densities⁷ to be around 60 meV. As an important final remark, the adatom-adatom interaction

was shown to decay slowly, with a repulsive ring past the short-range which may play an important role in the kinetics⁷.

In the present work we model the second monolayer of Ag on Ag/Pt(111), referred to as Ag/Ag/Pt(111). We use a generalization of the renowned 2D Frenkel-Kontorova (FK) model^{8,9}. This model has provided accurate and insightful analysis of similar reconstruction processes, such as Pt(111)¹⁰ or the first layer of Ag on Pt(111)¹¹. Our model differs from the standard FK in the following aspects. First of all, the substrate potential is vertically extended, i.e., it becomes a function of x , y and z . This way, the film is allowed to relax the stress by (small) vertical displacements of the atoms in the top-most Ag layer¹². A second difference is that the number of neighbours of any atom is not fixed beforehand, i.e., no topology is assumed. Thus, all kinds of lattice defects are allowed in the surface structure.

The substrate potential for the extended FK model is obtained by choosing a physically sensible general form and obtaining its parameters using *ab initio* density functional theory (DFT). For the film potential, we use a Morse type pair potential. The obtention of the minimum energy configurations of the extended FK model is a complex problem, which has been approached using the recently developed *replica-pinned quantum annealing* (RPQA)¹³.

The minimum energy configurations of the extended FK model are assumed to be (local) equilibrium atomic patterns of the reconstructed surface. Of course, this approach neglects the kinetic effects which may be relevant in the determination of the experimental configurations. We will provide some comments about these effects in section IV.

This article is organized as follows. Section II discusses the DFT calculations and the obtention of the extended FK model. The results of the numerical minimization are given in section III, while its physical interpretation

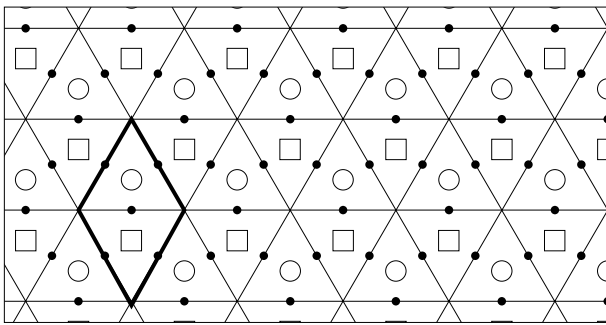


FIG. 1: Geometry of the Ag/Pt(111) system: top sites are shown as the vertices of the triangular network; FCC, HCP and bridge sites are shown as empty circles, empty squares and filled dots respectively. A unit cell is marked with a thicker line.

is provided in section IV, along with the most promising lines for further work.

II. MODEL

The behavior of an Ag monolayer on the Ag/Pt(111) system is simulated by an extended FK model, defined by the following functional form

$$E(\{r_i\}) = \sum_i V_s(r_i) + \sum_{\langle i,j \rangle} V_f(|r_i - r_j|) \quad (1)$$

where $r_i = (x_i, y_i, z_i)$ is the 3D position vector of the i^{th} Ag atom, V_s denotes the *substrate potential*, V_f is the *film potential*, and the sum over pairs $\langle i, j \rangle$ is extended over neighbours within a certain *cutoff* distance. This cutoff distance is determined so as to include the ring of first NN atoms. The vertical extension of the substrate potential¹² allows for stress relaxation via small vertical displacements along z -direction.

The appropriate intensive magnitude to minimize is, of course, the *energy per unit area*. The unit cell is shown by a bold line in Figure (1). The atomic density at the surface is, therefore, another relevant parameter to be obtained in our method.

Let us review concisely the geometry of our model. There are four types of distinguished points on the substrate lattice, which are known as FCC, HCP, top and bridge, as shown in Figure 1. The local equilibrium positions for an atom are the FCC and HCP, being the first slightly favoured energetically. Bridge sites are saddle-points (usually denoted with the letter p), and top positions, so called because they stand exactly above the substrate atoms, are strongly disfavoured energetically.

A. Density Functional Theory calculations

The parameters in the substrate potential are obtained using *ab initio* density functional theory (DFT) calcula-

tions with the pseudopotential approach and plane waves basis, as implemented in Quantum-Espresso¹⁴. We use generalized gradient approximation (GGA) for the exchange correlation interaction with the functional proposed by Perdew, Burke and Ernzerhof¹⁵. A kinetic energy cut-off of 367.2 eV and a higher cut-off of 2940 eV is used for the augmentation charges introduced by the ultrasoft pseudopotential¹⁶. To improve the convergence, a gaussian smearing of width 0.68 eV was adopted. Brillouin zone integrations for the (1×1) surface cell, shown by a thick line in Figure 1, were carried out using a $(15 \times 15 \times 1)$ mesh of k -points.

We obtained the bulk lattice parameter for Ag and Pt as 4.17 and 4.0 Å respectively, which give a misfit of 4.25%. These values compare well with the experimental values, 4.09 and 3.92, with a misfit of 4.33%, and the previous theoretical calculations of 4.19 Å and 4.01 Å⁶. According to our values, the nearest neighbour (NN) distance for Ag and Pt on the (111) surface are 2.95 and 2.83 Å respectively.

B. Substrate potential

The *substrate potential* $V_s(r)$ must share the periodicity of the substrate lattice, i.e., it will take the form of a Fourier series¹¹,

$$V_s(\mathbf{r}, z) = V_0 + \sum_{\mathbf{G}} V_{\mathbf{G}}(z) e^{i\mathbf{G} \cdot \mathbf{r}}, \quad (2)$$

where \mathbf{G} are 2D-vectors of the reciprocal substrate lattice and $\mathbf{r} = (x, y)$. This series is truncated arbitrarily to contain the first two shells of \mathbf{G} vectors, of length $4\pi/\sqrt{3}a_{\text{Pt}}$ and $4\pi/a_{\text{Pt}}$, separated by $2\pi/3$ rad, with $a_{\text{Pt}} = 2.83$ Å. The dependence on z is restricted to the coefficients $V_{\mathbf{G}}(z)$. When we expand equation (2) in the $V_{\mathbf{G}}$'s using the first two shells of \mathbf{G} vectors and apply the symmetries of the surface, we get an equation with four unknowns¹⁷. In order to obtain these four unknowns, we need to know the values of the substrate potential (V_s) at four non-equivalent positions on the surface, which we choose to be the FCC, HCP, bridge and top sites. Thus, we express the substrate potential $V_s(\mathbf{r})$ in terms of V_{FCC} , V_{HCP} , V_p , V_{top} . These values are calculated within DFT for a monolayer of Ag on a Ag/Pt(111) slab. The Ag/Pt(111) slab is simulated using a symmetric slab of seven Pt layers and one Ag layer adsorbed on both sides of Pt. We first calculate the equilibrium heights by relaxing the Ag monolayer on Ag/Pt(111) along the z -direction at the four sites. We use a vacuum width of 8 layers (18.47 Å) between the two Ag/Ag/Pt(111) slabs with the in-plane lattice parameter of 2.83 Å. Since the $V_{\mathbf{G}}$'s are functions of z , we calculate the energy of the second ML of Ag at various values of z by keeping the monolayer at different heights from the substrate. In this way, four functions of z are obtained: $\tilde{v}_k(z)$, with $k \in \{\text{FCC}, \text{HCP}, p, \text{top}\}$, by fitting the DFT results to a Morse-like form:

| | FCC | HCP | bridge | top |
|-----------------|---------|---------|---------|---------|
| z_{eq} (Å) | 2.45926 | 2.45977 | 2.54478 | 2.80834 |
| E_{min} (meV) | 0 | 3.638 | 35.2784 | 174.066 |

TABLE I: Equilibrium heights (z_{eq}) and corresponding energies to create a stacking fault in the second ML of Ag with respect to lowest energy FCC site, as obtained from DFT.

| z (Å) | E (FCC) | E (HCP) | E (bridge) | E (top) |
|---------|---------|---------|------------|---------|
| 2.27447 | 21.3928 | 26.7308 | 69.2716 | 326.563 |
| 2.64406 | 17.4284 | 19.2576 | 42.4184 | 192.134 |
| 2.73646 | 34.4624 | 36.7064 | 57.6368 | 178.520 |
| 3.34878 | 252.375 | 253.416 | 254.735 | 269.606 |

TABLE II: Energy (in meV) of an Ag atom on each of the four types of sites, at some values of z , with respect to the energy of the atom at its equilibrium height on FCC, as obtained with DFT.

$$\tilde{v}_k(z) = \frac{A_k}{\mu_k - \nu_k} \left(\nu_k e^{-\mu_k(z-z_k)} - \mu_k e^{-\nu_k(z-z_k)} \right) + V_{k,0} \quad (3)$$

where $\nu_k = \mu_k/2$. The substrate potential is now well defined from *ab initio* calculations.

If we evaluate the substrate potential at the equilibrium height of the FCC position, we should obtain the chemical potential for the Ag/Ag/Pt(111) system, μ , i.e., the energy required to take a single Ag adatom from its equilibrium position on the surface to infinity. We have estimated μ from DFT calculations as three times the binding energy of two Ag atoms in bulk. Thus, $\mu = 1.251$ eV.

Table I gives the equilibrium heights calculated from DFT at each type of site, along with the energy required to create a stacking fault relative to that of the FCC position. The value for the energy difference between the FCC and the HCP sites is consistent with the previous values given in the literature, about 3 meV. The energy barrier between them is lower in our case, about 35 meV, as compared to the 60 meV of other sources^{6,7}. The reason for this discrepancy is that they have done calculations on a single adatom adsorbed on FCC or bridge sites, whereas we use one full monolayer of Ag on Ag/Pt. Using a single adatom on FCC or bridge sites would obviously increase the binding energy of the adatom due to its lower coordination on the surface with respect to a full monolayer.

Some DFT data for the dependence on z of the substrate potential are given in Table II. A plot of $V_s(r) - \mu$ is shown in Figure 2. We would like to remark that the fit of $V_s(r)$ includes more points than those shown in table II (between 5 and 8 per site type), but only those are shown because they are computed for equal values of z .

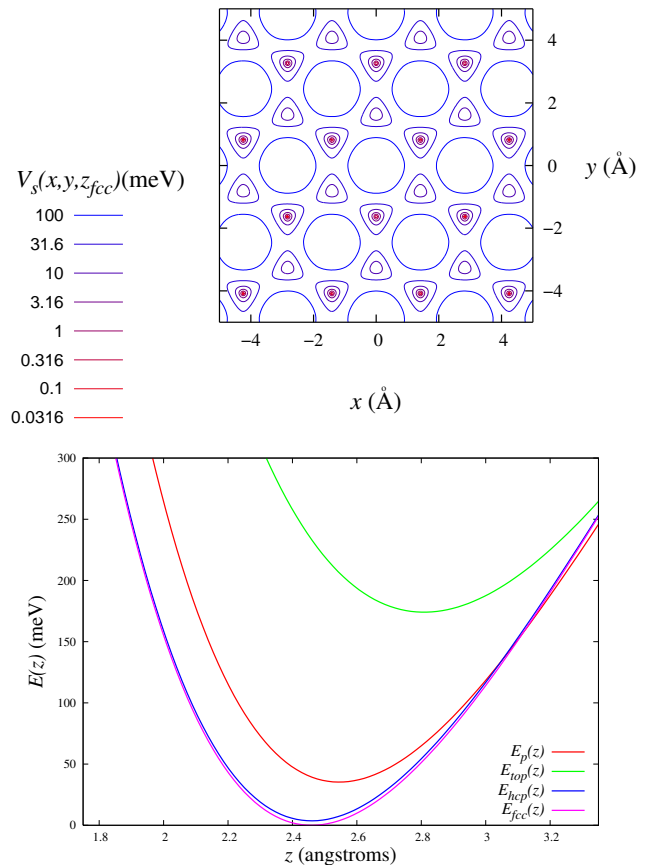


FIG. 2: (Color online) The substrate potential $V_s(r) - \mu$. Upper: contour plot of $V_s(x, y, z_{fcc}) - \mu$ calculated at the equilibrium height of the FCC sites. Lower: vertical dependence of the substrate potential, for the FCC, HCP, top and bridge sites.

C. Film potential

The film potential $V_f(r)$ (also known as *surface potential*) simulates the interaction among Ag atoms in the Ag layer on Ag/Pt(111) surface. We assume it to be an isotropic pair potential of Morse type.

$$V_f(r) = a_0 \left[\left(1 - e^{-a_1(r-b)} \right)^2 - 1 \right] \quad (4)$$

In this equation, b is the equilibrium distance, a_0 the depth of the potential well and a_1 the curvature around the minimum. However, $V_f(r)$ is rather difficult to obtain from DFT calculations due to the heteroepitaxial nature of the problem. The closest approximation would be to calculate it for Ag atoms on a Ag(111) surface. However, the nearest neighbour (NN) distance in the Ag layer on Ag/Pt(111) surface is 2.83 Å, while the NN atomic distance in the Ag layer on Ag(111) surface is 2.95 Å. Therefore, as one would expect, Ag layer on Ag/Pt(111) surface is under compressive stress of 0.198 eV/Å² and Ag layer on Ag(111) surface is under tensile stress of 0.091

eV/Å². Due to this difficulty, we have fixed the value of b to 2.95Å, i.e., the lattice parameter of Ag, and run simulations for different values of a_0 and a_1 , as we will see in the next section.

In order to calculate the total film energy, we only consider pairs of atoms closer than a certain cutoff distance $d_{\text{cutoff}} = 6\text{Å}$. As a technical side remark, we added a tiny constant to the potential in order to avoid a discontinuity at that distance. Therefore, the topology of the epilayer is not fixed beforehand: the number of neighbours of a given atom is not restricted.

The Ag-Ag pair potential has a complex structure at longer distances, which we have neglected in this work. Other authors⁷ have shown the effect of Friedel-like oscillations at long distances, recognizing a ring of repulsion in the pair potential. This ring is beyond our cutoff distance and we will assume it to be negligible in order to determine the equilibrium configuration. Its effects on the kinetics of the system might be much more pronounced, and will be discussed in section IV.

III. OPTIMUM CONFIGURATIONS

A. Numerical optimization

Once the extended FK Hamiltonian has been determined, i.e., the substrate and film potential have been found, the main task is to obtain the positions of the Ag atoms which minimize the total energy, i.e., its equilibrium configuration.

Global optimization of a potential energy surface (PES) with a large amount of local minima is a highly non-trivial task. Simulated thermal annealing is one of the most popular non-biased general-purpose optimization methods, in which thermal fluctuations allow the system to escape metastable states in order to achieve the real global minimum. A recent innovation is that of *simulated quantum annealing*, in which quantum fluctuations collaborate with thermal fluctuations in this task^{18,19}. Using path integral concepts, the original system is replaced by a set of *replicas* exploring the same PES, linked among themselves with springs of zero natural length, at a fictitious finite temperature. *Replica-pinned quantum annealing* (RPQA) is a technical variant which has provided the best non-biased results to date for the determination of the global minimum energy structures of Lenard-Jones clusters. The basic idea is to update all replicas *excluding* the one which has reached the best energy so far. The details can be found in the original article by Gregor and Car¹³.

The application of the RPQA to the obtention of the global minimum of FK models is one of the main technical improvements developed in this work. Both in 1D and in 2D, the efficiency of the method is higher than the case of simulated thermal annealing. RPQA tends to explore more thoroughly the area around the best replica so far, thus removing defects faster than other methods.

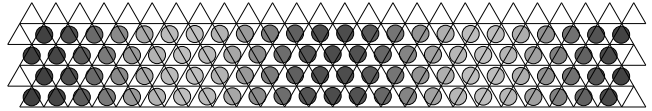


FIG. 3: Top view of the striped reconstruction of the Ag/Ag/Pt(111) surface, on a 25×4 unit cell. Notice the wavy pattern, with a wavelength of $\approx 25a_{\text{Pt}}$. Heights are denoted by the shades of gray: the darker the atom, the lower its height.

Detailed results and comparisons will be provided elsewhere.

Of course, it is impossible in these problems to be completely sure that the best minimum obtained is the true global minimum, but after an exhaustive search and coincidence of diverse methods a large degree of confidence can be assumed.

B. Results

An exhaustive search for the minimum energy configurations of the extended FK model, as defined in equation 1, has been carried out using the procedure described in the previous section. For all the simulations, we use periodic boundary conditions (PBC), with different sizes for the system cell. A few important parameters were systematically varied. On one hand, the parameters a_0 and a_1 , i.e., the depth and curvature of the film potential, for which *ab initio* methods have not provided a reliable estimate. On the other hand, the atomic density of the surface, i.e., the number of particles per unit area.

Among the huge number of local minima, we have selected three of them because of their special physical relevance. They are local minima of the PES for all reasonable values of a_0 and a_1 .

- (a) **Unreconstructed configuration.** The homogeneous configuration in which all Ag atoms stay in the FCC positions on Ag/Pt(111). The surface is under compressive stress.
- (b) **Striped configuration.** In this configuration the stress is relaxed by placing some particles in HCP positions, as shown in Figure (3) (25×4 unit cell with 24×4 Ag atoms). The increase of substrate energy is compensated by the decrease in the film energy due of the stretching of the horizontal links. The wavy pattern established has a preferred wavelength, of approximately $25a_{\text{Pt}}$. Thus, there is a decrease of density as compared to the first Ag ML, of 4%.
- (c) **Triangular configuration.** Stress is relaxed in an isotropic way, creating lines of defects following the symmetry axes of the substrate, as it is shown in Figure 4. The density of this configuration decreases by 7.8% with respect to the unreconstructed

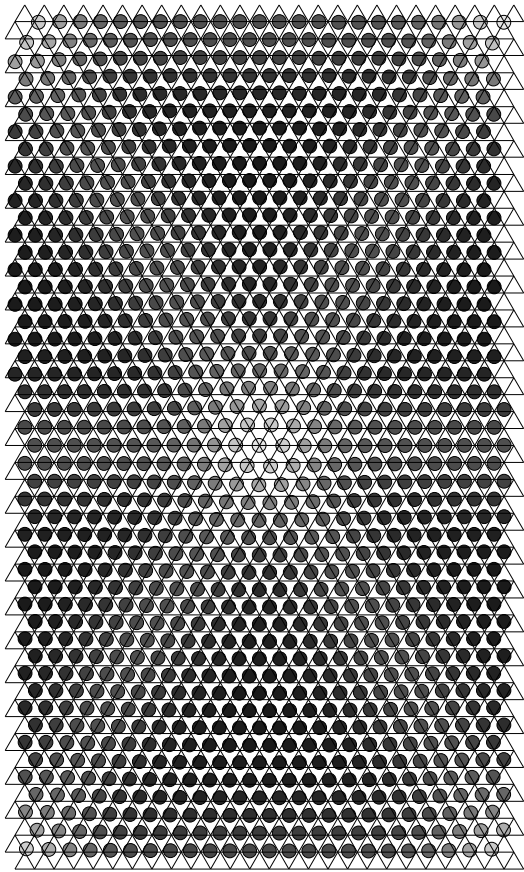


FIG. 4: Top view of the triangular reconstruction of Ag/Ag/Pt(111) surface. Heights are denoted by the shades of gray: the darker the atom, the lower its height.

case. In order to allow the relaxation of the surface bonds, some atoms must stay close to top sites.

Which of them is the global minimum of the PES depends on the values of a_0 and a_1 . Figure 5 depicts a phase diagram in which the stable configuration is shown as a function of these two parameters.

The striped configuration is reported experimentally by Brune and coworkers⁴. According to their work, under annealing at 800 K, it relaxes to another configuration which is similar to our triangular configuration. It is well known that, under annealing, the system is much more likely to find the global energy minimum of the PES. Therefore, the experimental data imply that the triangular structure is, indeed, that global minimum, while the striped configuration is a long-lived metastable state, i.e.: a local minimum. The reasons for its long lifetime are a large energy barrier and a small difference in energies between both configurations.

Therefore, the numerical data are compatible with the experimental results in as much as the values of a_0 and a_1 are close to the curve which separates the striped and the triangular regions in the phase diagram of Figure (5). The precise point within that curve can not be determined from our calculations.

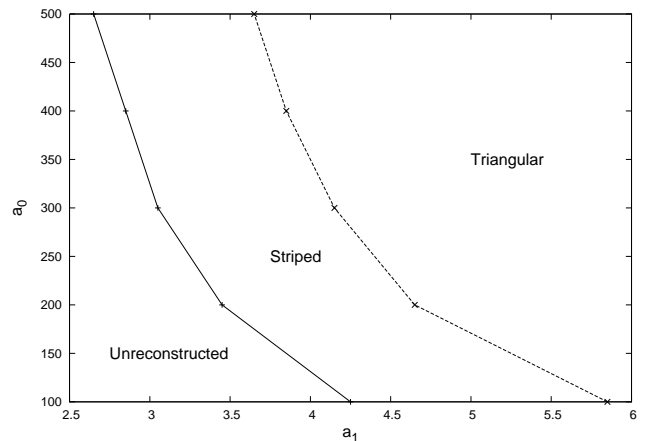


FIG. 5: Phase diagram which shows the global minimum of the PES as a function of the parameters of the film potential, a_0 and a_1 .

IV. DISCUSSION AND FURTHER WORK

Our theoretical model shows from *ab initio* calculations, that the Ag/Ag/Pt(111) can reconstruct into a striped or a triangular configuration for some choices of its free parameter (a_0 and a_1 in the film potential). Both the equilibrium and the metastability situations can be explained satisfactorily.

The fact that the striped configuration is preferred *before annealing* requires further clarification. It must have a larger energy per unit cell than the triangular structure, but kinetic effects may make it more likely to appear. A full theoretical explanation of this fact remains as an open task, but we may already make some remarks with the available information. At room temperature, Ag adatoms on the Ag/Pt(111) surface will not distinguish clearly between HCP and FCC sites. The repulsion ring described by Fichthorn and Scheffler⁷ explains the formation, at low coverages, of a high amount of small islands surrounded by an *exclusion area* which makes it difficult for other adatoms to join. With the energy difference of 3 meV between FCC and HCP sites, we can predict that, at room temperature, roughly 50% of these islands will be on each type of site. Islands will merge slowly, and some domain boundaries will appear. At moderate coverages, the most likely configuration for these domain boundaries is a set of parallel lines, giving rise to the striped configuration. The complex network which is characteristic of the triangular configuration will be more unlikely, although it leads to a lower energy for a complete layer.

There are some differences between the global minimum with triangular symmetry obtained in this work and the configuration reported by Brune and coworkers. In the later structure, no atoms sit on bridge or top sites. With our PES, the energy per unit cell of that configuration is higher than the energy of the unreconstructed surface. When we use this structure as the starting configuration for our quantum annealing minimization al-

gorithm, the system relaxes to our triangular structure. A thorough search has been performed in the parameter space in order to obtain the structure of Brune and coworkers as the global minimum of the PES, without success. This could mean that, we will have to abandon the Frenkel-Kontorova approximation in order to obtain the experimental configuration as a global minimum of a PES. The assumption which is most likely to fail is the independence of the film potential from the coordination number. The lower coordination of some sites increases the strength with which they bind to their neighbours. This effect is taken into account in other more complex models, such as the glue model²⁰.

Other systems which are of interest, where our vertically extended Frenkel-Kontorova model can provide insight are the reconstruction of similar metallic surfaces, such as Cu/Ru(1111). Surface growth in semiconductors, such as the Stranski-Krastanov growth mode in InAs/GaAs will require major modifications, since isotropy of the film potential might not be an acceptable approximation. On the other hand, the vertical exten-

sion could prove much more useful in this case, where the film tends to really curve.

On the computational side, this work applies quantum annealing methods to a physical problem with experimental comparison, i.e., not just a benchmark problem^{13,18,19}. Of course, quantum annealing should not be considered as the panacea for all optimization problems. It is just another tool in our numerical toolbox, which can prove useful in a variety of cases.

Acknowledgments

The authors would like to acknowledge Shobhana Narasimhan and Stefano de Gironcoli for very useful discussions, and also to the Scuola Internazionale Superiore di Studi Avanzati (SISSA, Trieste, Italy), where this work was started. This work has been partly supported by the Spanish government through project FIS2006-04885 (J.R.-L.).

-
- ¹ J. V. Barth, H. Brune, G. Ertl, and R. J. Behm, *Phys. Rev. B* **42**, 9307 (1990).
- ² S. Narasimhan and D. Vanderbilt, *Phys. Rev. Lett.* **69**, 1564 (1992).
- ³ H. Brune, H. Röder, C. Boragno, and K. Kern, *Phys. Rev. B* **49**, 2997 (1994).
- ⁴ H. Brune, H. Röder, C. Boragno, and K. Kern, *Phys. Rev. B* **49**, 2997 (1994).
- ⁵ H. Brune, M. Giovannini, K. Bromann, and K. Kern, *Nature* **394**, 451 (1998).
- ⁶ C. Ratsch, A. Seitsonen, and M. Scheffler, *Phys. Rev. B* **55**, 6750 (1997).
- ⁷ K. A. Fichthorn and M. Scheffler, *Phys. Rev. Lett.* **84**, 5371 (2000).
- ⁸ O. M. Braun and Y. S. Kivshar, *The Frenkel-Kontorova model* (Springer Verlag, 2004).
- ⁹ J. Frenkel and T. Kontorova, *J. Phys. USSR* **1**, 137 (1939).
- ¹⁰ R. Pushpa and S. Narasimhan, *Phys. Rev. B* **67**, 205418 (2003).
- ¹¹ J. Hamilton, R. Stumpf, K. Bromann, M. Giovannini, K. Kern, and H. Brune, *Phys. Rev. Lett.* **82**, 4488 (1999).
- ¹² J. Rodriguez-Laguna and S. N. Santalla, *Phys. Rev. B* **72**, 125412 (2005).
- ¹³ T. Gregor and R. Car, *Chem. Phys. Lett.* **412**, 125 (2005).
- ¹⁴ S. Baroni, A. D. Corso, S. de Gironcoli, and P. Giannozzi (<http://www.Quantum-Espresso.org>, 2003).
- ¹⁵ J. P. Perdew, K. Burke, and M. Ernzerhof, *Phys. Rev. Lett.* **77**, 3865 (1996).
- ¹⁶ D. Vanderbilt, *Phys. Rev. B* **41**, 7892 (1990).
- ¹⁷ R. Pushpa, Ph.D. thesis, Jawaharlal Nehru Centre for Advanced Scientific Research, India (2005).
- ¹⁸ A. Das and B. K. Chakrabarti, *Quantum Annealing and Related Optimization Methods*, Lecture Notes in Physics (Springer Verlag, 2005).
- ¹⁹ Y.-H. Lee and B. Berne, *J. Phys. Chem. A* **104**, 86 (2000).
- ²⁰ F. Ercolessi, E. Tosatti, and M. Parrinello, *Phys. Rev. Lett.* **57**, 719 (1986).